AIAA JOURNAL
Vol. 46, No. 5, May 2008

Starting Pressure and Hysteresis Behavior of an Annular Injection Supersonic Ejector

Sehoon Kim*
Agency for Defense Development, Daejeon 305-600, Republic of Korea
and
Sejin Kwon†
Korea Advanced Institute of Science and Technology, Daejeon 305-701, Republic of Korea

DOI: 10.2514/1.22363

An analytical model to predict the primary stagnation pressure that starts an annular injection supersonic ejector is presented. If the length of the mixing chamber is longer than the critical length, the starting pressure increases proportionally to the mixing chamber length, which differs from conventional ejectors using central injection. To describe the dependency of the starting pressure on the mixing chamber length, we assume that the ejector starts when the exiting supersonic primary flow reaches the second throat. In the present model, we use a subsonic mixing model to calculate the secondary flow pressure in the mixing chamber. Applying the obtained pressure as a back pressure condition, the distance that the supersonic primary flow develops is calculated. Comparing the distance to the mixing chamber length, we derive a minimum pressure requirement diagram that accurately predicts the starting pressure and hysteresis for a given geometry.

Nomenclature

A	=	cross-sectional area, mm^2
D	=	diameter, mm
h	=	specific enthalpy, J/kg
L	=	length, m
M	=	Mach number
MW	=	molecular weight, g/mol
m	=	mass flow rate, kg/s
P	=	pressure, bar
R	=	gas constant, J/kgK
S	=	empirical factor
T	=	temperature, K
v	=	velocity, m/s
α	=	contraction angle of mixing chamber, deg
γ	=	specific heat ratio
δ	=	expansion angle of diverging section, deg
η_d	=	efficiency of subsonic diffuser
λ	=	first period length of diamond-shaped shock of overexpanded flow
ρ	=	density, kg/m^3

Subscript

0	=	stagnation state
2	=	second throat
a	=	ambient condition
b	=	back pressure
cr	=	critical length of mixing chamber
d	=	diverging section of diffuser
e	=	ejector exit
i	=	mixing chamber inlet
m	=	second-throat inlet (complete mixing condition)
max	=	outer diameter of primary nozzle exit
P	=	primary flow
S	=	secondary flow
st	=	starting condition
unst	=	unstarting condition

Received 10 January 2006; revision received 5 October 2007; accepted for publication 8 December 2007.

*Senior Researcher, Jochiwangil 462, Yuseong-gu. Member AIAA.
†Associate Professor, Department of Mechanical Engineering and Division of Aerospace Engineering, KAIST, 373-1 Guseong-dong, Yuseong-gu. Member AIAA.

I. Introduction

HIGH performance supersonic ejectors are generally equipped with a diffuser for pressure recovery with minimal loss before the flow is dumped to the ambient [1–3]. In many applications of supersonic ejectors, such as high-altitude test facilities [4–8], pressure recovery systems for high-power chemical lasers [9,10], thermocompressors in desalination plants [11], and ejector ramjets [12–14], the stagnation pressure of the primary flow that starts the ejector is an important design parameter. The starting pressure can be lowered by attaching a converging–diverging diffuser downstream from the ejection location [3]. The converging section of this diffuser is commonly called the mixing chamber, as the supersonic primary flow and subsonic secondary flow mixes within this region. Because of the interaction with the subsonic secondary flow, the supersonic primary flow is decelerated. When the stagnation pressure of the primary flow is not high enough, subsonic mixing occurs in the mixing chamber and the mixed flow enters the second throat at a subsonic speed. If the flow entering the second throat is supersonic, the ejector starts abruptly and a very low secondary flow pressure can be obtained [1].

A supersonic ejector equipped with a converging–diverging diffuser is known to exhibit hysteresis behavior in its performance curve, as shown in Fig. 1 [3]. The performance curve plots the static pressure of the secondary flow as a function of the stagnation pressure of the primary flow. The horizontal and vertical axes in the plot represent the stagnation pressure of the primary flow and the static pressure of the secondary flow, respectively, normalized by atmospheric pressure. As the stagnation pressure of the primary flow increases, the static pressure of the secondary flow decreases from its initial stagnation pressure, which is atmospheric when the secondary flow is drawn from the ambient, as in the present case. Therefore, the secondary flow is being accelerated in region 1 of the plot, but the flow outside of the primary nozzle remains subsonic. When the stagnation pressure of the primary flow further increases into

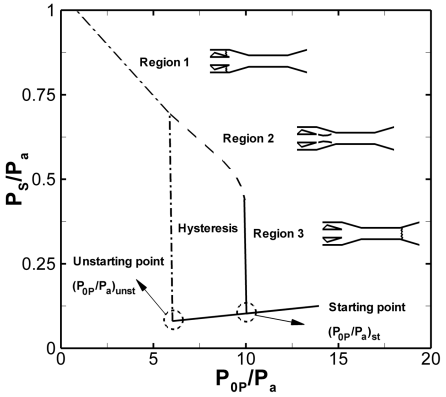

Fig. 1 Performance curve of a typical annular injection supersonic ejector equipped with a second throat.

region 2, the supersonic region extends out of the primary nozzle but the entire mixing chamber is not supersonic. As the primary stagnation pressure reaches the starting pressure in region 3, the normal shock wave is suddenly swallowed by the second throat and moves to the diverging section of the diffuser. At this moment, the secondary flow is aerodynamically choked by the interaction with the primary supersonic flow, and the entire mixing chamber is filled with supersonic flow. The minimum stagnation pressure of the primary flow that starts the ejector is called the starting pressure. Once the ejector has started, the ejector is in full operation, even for a primary stagnation pressure below the starting pressure. The same phenomenon is also observed in a closed supersonic wind tunnel with a second throat [15,16]. By taking advantage of the hysteresis, the operating pressure of the primary flow can be reduced significantly.

Kim et al. [3] investigated the effects of the geometric parameters of an annular injection supersonic ejector on the ejector's performance, including the starting and unstarting pressures of the primary flow. In their results, the unstarting pressure is linearly proportional to the throat area ratio of the second throat to the primary nozzle, and it can be calculated simply using the normal shock theory with the throat area ratio, as is also widely used in conventional central injection supersonic ejector design [6–8]. Kim et al. [3] also demonstrated that the gap between the starting and unstarting pressures increases as the length of the mixing chamber increases. If the mixing chamber is shorter than the critical length, the starting pressure is identical to the unstarting pressure and there is no hysteresis. Whereas when the mixing chamber is longer than the critical length, the starting pressure increases in proportion with the length of the mixing chamber and the performance curve shows obvious hysteresis behavior. The hypothetical critical length is defined as the length of the flow passage over which the flow is supersonic for a given inlet condition.

Hysteresis behavior can be seen in annular injection ejectors more often than in conventional central injection ejectors because the contraction angle should be small enough to reduce the pressure loss caused by the oblique shock wave originating from the mixing chamber inlet. Therefore, the annular injection supersonic ejector naturally has a long mixing chamber.

Figure 2 shows the typical configuration of an annular injection supersonic ejector with a second throat. The mixing chamber length increases as the contraction angle, α, decreases for a fixed outer diameter, $D_{\max}$. This type of ejector, nowadays, is used when the secondary flow temperature is remarkably high, as in high-altitude test facilities [4–8] and pressure recovery systems of chemical lasers [9,10] for the thermal safety of the structure inside the ejector. Therefore, the prediction of the starting pressure of an annular injection supersonic ejector is important.

II. Theoretical Analysis

The starting and unstarting mechanism of a supersonic ejector with a converging–diverging diffuser is complex and not yet fully understood. The process is intrinsically unsteady and involves supersonic turbulent mixing between the primary and secondary flows. In the present study, a simple theoretical model to predict the starting stagnation pressure of the primary flow is proposed. We assume that the supersonic ejector starts when the flow downstream from the primary nozzle becomes completely supersonic up to the second-throat inlet. While the stagnation pressure of the primary flow is less than the starting pressure, the secondary flow pressure does not decrease sufficiently and the flow exiting the primary nozzle remains overexpanded as schematically depicted in Fig. 3. One criterion to start the ejector is the distance that the primary exit flow penetrates at a supersonic speed into the mixing chamber. If this distance is greater than the mixing chamber, the ejector starts.

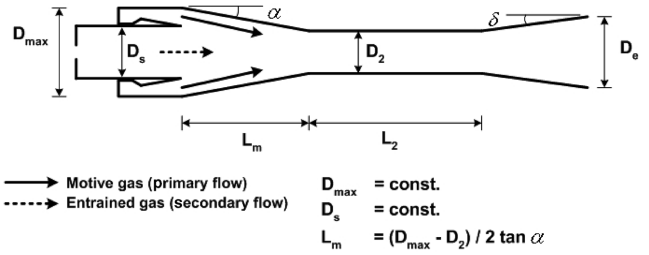

Fig. 2 Schematic of an annular injection supersonic ejector.

The primary flow discharging into the mixing chamber is illustrated in Fig. 4. Because of the overexpansion of the primary flow, a series of oblique shock-expansion waves will develop downstream from the primary exit. Let λ be the distance that the first series of oblique shock-expansion waves occupies. Then, the distance of the supersonic primary exit flow will be $S\lambda$, where S is an empirical factor. We will explain the S factor more in Sec. II.B.

The prediction of the starting pressure is calculated using two steps. First, the static pressure of the secondary flow is calculated assuming that the primary and secondary flows are completely mixed at the second-throat inlet. In this calculation, the mixed flow passes through the second throat isentropically, and further subsonic deceleration takes place in the diverging section. Second, by assigning the calculated pressure of the secondary flow to the back pressure of the primary flow, the distance that the primary flow penetrates into the mixing chamber at supersonic speed is calculated. A rigorous calculation of this distance would eliminate the merit of the simple analysis of the present study; therefore, an approximate estimation of this distance will be used. These calculations result in a plot that correlates the mixing chamber length and the minimum stagnation pressure of the primary flow that is required to start the ejector.

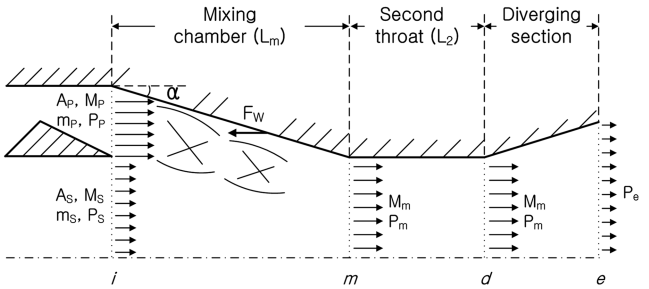

Fig. 3 Schematic of the mixing model with notations of variables.

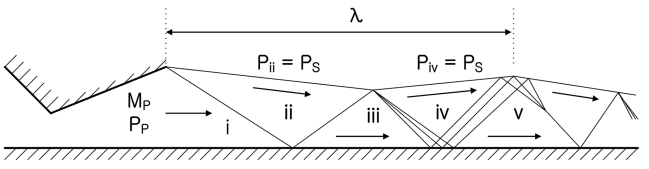

Fig. 4 Schematic of the diamond-shaped shock wave pattern formed in the exhaust from a supersonic nozzle.

A. Mixing Model

To analyze the flowfield in the mixing chamber, we applied the subsonic mixing model [17]. A detailed diagram of the mixing chamber is shown in Fig. 3. The primary and secondary flows enter the mixing chamber at i with known flow properties. The completely mixed flow enters the second throat at m at subsonic speed. The diverging section, d–e, further slows the flow isentropically. The control volume is bounded by inlet i, exit m, the mixing chamber wall, and the axis of symmetry. The conservation equations for mass, momentum, and energy are expressed as follows:

$$m_P + m_S = m_m \tag{1}$$

$$P_P A_P + P_S A_S - P_m A_m - F_W = -v_P(\rho_P A_P v_P) - v_S(\rho_S A_S v_S) + v_m(\rho_m A_m v_m) \tag{2}$$

$$\left(h_P + \frac{v_P^2}{2}\right)m_P + \left(h_S + \frac{v_S^2}{2}\right)m_S = \left(h_m + \frac{v_m^2}{2}\right)m_m \tag{3}$$

F_W is the reaction force at the mixing chamber side wall and is evaluated by the following equation. For simplicity, we used the average pressure of the primary nozzle exit pressure, P_P, and the second-throat inlet pressure, P_m.

$$F_W = \frac{P_P + P_m}{2}(A_P + A_S - A_m) \tag{4}$$

Using the equation of the state for ideal gas, the definitions of Mach number, and the speed of sound, Eqs. (1) and (2) can be expressed in terms of Mach numbers, as follows:

$$\frac{m_m}{m_P} = 1 + \frac{m_S}{m_P} = \frac{P_m}{P_P}\cdot\frac{A_m}{A_P}\left[\frac{MW_m}{MW_P}\cdot\frac{T_{0P}}{T_{0m}}\right]^{1/2} \cdot \frac{M_m\{\gamma_m[1+\frac{\gamma_m-1}{2}M_m^2]\}^{1/2}}{M_P\{\gamma_P[1+\frac{\gamma_P-1}{2}M_P^2]\}^{1/2}} \tag{1a}$$

$$P_P A_P\left(1+\gamma_P M_P^2\right) + P_S A_S\left(1+\gamma_S M_S^2\right) = P_m A_m\left(1+\gamma_m M_m^2\right) + \frac{P_P + P_m}{2}(A_P + A_S - A_m) \tag{2a}$$

By eliminating P_m from these two equations, we can obtain a simple expression for M_m. To simplify the mathematical expression of the equation to Eq. (5), three gasdynamic functions were introduced [17].

The specific heat ratio (γ_m) is calculated by taking the mass weighted average of the respective properties at the second-throat inlet, and the stagnation temperature (T_{0m}) of the mixed flow is obtained by applying the thermodynamic relations to the energy equation [17,18].

$$\gamma_m = \frac{\frac{m_S}{m_P}\cdot\frac{MW_P}{MW_S}\cdot\left(\frac{\gamma_S}{\gamma_S-1}\right) + \left(\frac{\gamma_P}{\gamma_P-1}\right)}{\frac{m_S}{m_P}\cdot\frac{MW_P}{MW_S}\cdot\left(\frac{1}{\gamma_S-1}\right) + \left(\frac{1}{\gamma_P-1}\right)} \tag{9}$$

$$T_{0m} = \frac{T_{0S}\cdot\frac{m_S}{m_P}\cdot\frac{MW_P}{MW_S}\left(\frac{\gamma_S}{\gamma_S-1}\right) + T_{0P}\cdot\left(\frac{\gamma_P}{\gamma_P-1}\right)}{\frac{m_S}{m_P}\cdot\frac{MW_P}{MW_S}\cdot\left(\frac{\gamma_S}{\gamma_S-1}\right) + \left(\frac{\gamma_P}{\gamma_P-1}\right)} \tag{10}$$

With γ_m and T_{0m} given by Eqs. (9) and (10), Eq. (5) can be solved iteratively by guessing the secondary pressure, P_S, at i. Then, M_m can be obtained using the quadratic equation (8). Choosing between the two solutions of this quadratic equation, the M_m less than 1 is the true solution because the ejector has not yet started. The pressure of the mixed flow at m can be calculated by the momentum equation, Eq. (2). The mixed flow slows in the diverging section of the diffuser whose isentropic efficiency is η_d and discharges into the ambient air. Then, the pressure at the exit of the ejector (at location e) can be calculated by Eq. (11).

$$P_e = P_d\left(1 + \eta_d\cdot\frac{\gamma_m - 1}{2}\cdot M_d^2\right)^{\gamma_m/(\gamma_m-1)} \tag{11}$$

Equations (5–11) are calculated repeatedly until the diffuser exit pressure, P_e, is equal to the ambient pressure, P_a. The static pressure of the secondary flow is obtained when this condition is met.

B. *S* Factor for the Supersonic Primary Flow Distance

With the static pressure of the secondary flow obtained by the aforementioned calculation procedure, it is possible to estimate the distance over which the overexpanded primary flow develops. However, the estimation will take much time and effort without any guarantee of accuracy. In the present study, we only calculated the length of the first series of diamond-shaped wave patterns (from i to v), as shown in Fig. 4 [15,19]. Then, we used the calculated length as the characteristic length (λ) to obtain the distance over which the overexpanded primary flow develops by multiplying it by the empirical factor, S. This concept results from the hypothesis that the characteristic length shows the same dependency as the full distance of the overexpanded primary flow on the stagnation pressure of the primary flow. In other words, the full distance of the overexpanded primary flow can be described as $S\lambda$.

Although the S factor essentially results from considering the repetition of the diamond-shaped wave pattern, various physical phenomena that have not been adequately accounted for in this simplified model are included, that is, the contraction angle at the mixing chamber inlet, wall friction, and supersonic–supersonic interaction. However, the S factor is almost constant for similar sizes, such as the inner diameter at the primary nozzle exit, because all of these physics are strongly dependent on size, especially in an internal flow.

A large S factor indicates that the full distance of the overexpanded primary flow, $S\lambda$, is long, as shown in Fig. 5. If the mixing chamber is sufficiently long, that is, $L_m > S\lambda$, the primary flow becomes subsonic within the mixing chamber. Increasing the stagnation pressure, the minimum stagnation pressure that makes $L_m = S\lambda$ will

$$F_3(\gamma_m, M_m) = \frac{\frac{m_P A_m}{m_m}\cdot[F_1(\gamma_P, M_P) + \frac{P_S}{P_P}\cdot\frac{A_S}{A_P}F_1(\gamma_S, M_S) - \frac{A_P + A_S - A_m}{2A_P}]\cdot[\frac{MW_m}{MW_m}\cdot\frac{T_{0P}}{T_{0m}}]^{1/2} - \frac{1}{2}\cdot\frac{F_2(\gamma_P, M_P)}{F_2(\gamma_m, M_m)}(A_P + A_S - A_m)}{A_m F_2(\gamma_P, M_P)} \tag{5}$$

$$F_1(\gamma, M) = 1 + \gamma M^2 \tag{6}$$

$$F_2(\gamma, M) = M\left\{\gamma\left[1 + \frac{\gamma-1}{2}M^2\right]\right\}^{1/2} \tag{7}$$

$$F_3(\gamma, M) = \frac{F_1(\gamma, M)}{F_2(\gamma, M)} = \frac{1 + \gamma M^2}{M\{\gamma[1+\frac{\gamma-1}{2}M^2]\}^{1/2}} \tag{8}$$

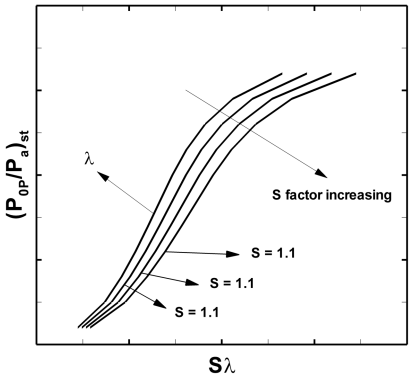

Fig. 5 The *S* factor effect.

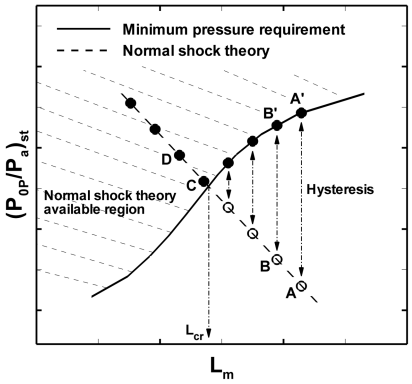

Fig. 6 Minimum pressure requirement diagram.

be the starting pressure. In the present study, the *S* factor was estimated from measurements taken by Kim et al. [3] in three different cases of primary nozzle area ratio.

C. Minimum Pressure Requirement Diagram

Figure 6 illustrates the relationships between the mixing chamber length and the stagnation pressure of the primary flow that starts the ejector. In the figure, the dashed line is the normal shock theory with the throat area ratio for a fixed contraction angle. In the configuration of the present study, the throat area ratio is a function of only the mixing chamber length, as shown Fig. 2, because $D_{\max}$ and the contraction angle are constant. The solid curve is the distance over which the overexpanded primary flow penetrates at a supersonic speed for a given stagnation pressure. In other words, it is the minimum stagnation pressure to start an ejector with an arbitrary mixing chamber length. For a given primary stagnation pressure, if the mixing chamber length is shorter than the solid curve, the starting pressure is obtained by the normal shock theory, as in cases C and D. On the other hand, a higher pressure is required to start the ejector, as in A′ and B′, when the chamber geometry is located below the solid line, such as in A and B. For a long mixing chamber, the stagnation pressure of the primary flow for the start of the ejector increases with the mixing chamber length. The hysteresis that is manifested by the difference between the stagnation pressures that start and unstart the ejector can be explained easily in the same way in this figure. The critical length of the mixing chamber (L_{cr}) is the interaction between the solid line and the dashed line in Fig. 6.

III. Results and Discussion

The analysis was applied to the annular injection supersonic ejector equipped with a converging–diverging diffuser tested by Kim et al. [3]. It was an air-to-air ejector. A schematic is shown in Fig. 2 and the detailed configurations are listed in Table 1. Tests were constructed for three different Mach numbers (3.8, 4.0, and 4.2) at the primary exit. At each Mach number, nine cases of mixing chamber

Table 1 Ejector configurations

Primary Mach number	3.8, 4.0, 4.2
Outer diameter of the primary nozzle exit, mm	44
Inner diameter of the primary nozzle exit, mm	34
Contraction angle of the mixing chamber, °	4, 7, 10
Second-throat diameter, mm	27, 28, 29
Second-throat L/D ratio	8
Diameter of the ejector exit, mm	50
Diverging angle of the diffuser, °	5

Table 2 Tested lengths of the mixing chamber

No.	α, °	D_2, mm	L_m, mm
1	——	27	121.6
2	4	28	114.4
3	——	29	107.3
4	——	27	69.2
5	7	28	65.2
6	——	29	61.1
7	——	27	48.2
8	10	28	45.4
9	——	29	42.5

geometries were examined and are listed in Table 2. The mixing chamber length, L_m, was determined by the contraction angle and the second-throat diameter as shown in Fig. 2. For a fixed outer diameter of the primary nozzle exit ($L_{\max} = 44$ mm), the mixing chamber length was controlled by changing the contraction angle and the second-throat diameter, as shown in Fig. 2. In all cases, the secondary mass flow rate was fixed at 2 g/s and the efficiency of the diverging section was assumed to be 75%. The inlet temperature was 300 K.

The minimum pressure requirement diagrams of the three Mach numbers at the primary exit are plotted in Figs. 7–9. For the *S* factors at 3.1, 3.05, and 3.0, all three cases showed good agreement with the measurements. The reason that the *S* factor decreases slightly with an increase in the Mach number at the primary exit is due to a lower static pressure of the secondary flow pressure corresponding to the Mach number. In other words, for a higher primary exit Mach number, a lower secondary flow pressure is obtained, and the supersonic primary flow can develop easily. Nevertheless, the difference is insignificant for ejectors of similar sizes. In each figure, when the contraction angle is 10 deg (points 7–9), the stagnation pressure of the primary flow that starts the ejector is inversely proportional to the mixing chamber length. This pressure is predicted by the normal shock theory based on the throat area ratio. However, if the contraction angle is 4 deg (points 1–3), the stagnation pressure of the primary flow that starts the ejector is proportional to the mixing chamber length. Furthermore, the switching of these contradicting behaviors was observed in points 4–6 in Figs. 7 and 8. From this

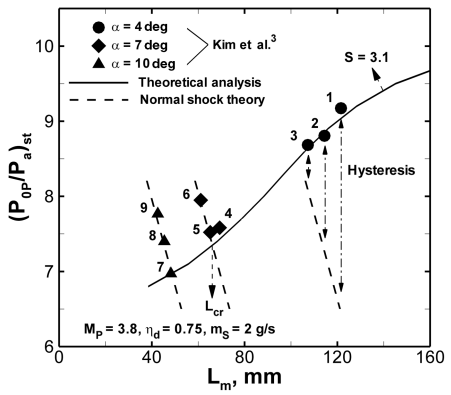

Fig. 7 Minimum pressure requirement diagram with the primary Mach number 3.8.

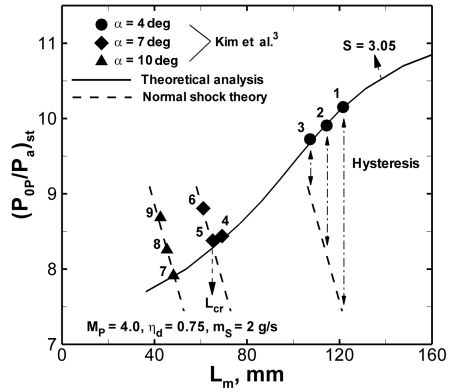

Fig. 8 Minimum pressure requirement diagram with the primary Mach number 4.0.

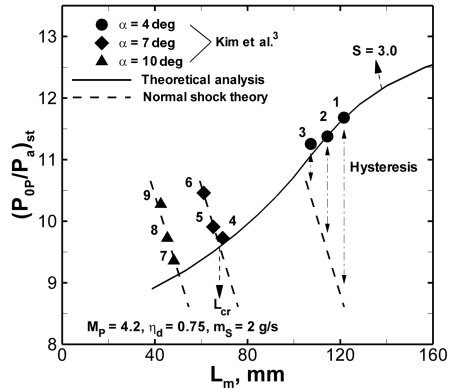

Fig. 9 Minimum pressure requirement diagram with the primary Mach number 4.2.

observation, Kim et al. [3] introduced the critical length for the mixing chamber to explain the switching of the correlation between the minimum pressure and the chamber length. According to the figures, we can see that the critical length can be obtained through the interaction of the minimum starting pressure curve and the prediction of the normal shock theory. The calculated critical length was compared with the measurements of Kim et al. [3] for different primary exit Mach numbers in Table 3; in all test cases, they showed good agreement. The stagnation pressure of the primary flow that unstarts the ejector is determined by the normal shock theory for a given throat area ratio. As a result, the gap between the stagnation pressure that starts and unstarts the ejector widens as the mixing chamber length increases from points 1 to 3 in Figs. 7–9.

IV. Conclusions

For an annular injection supersonic ejector equipped with a converging–diverging diffuser, the starting pressure is linearly proportional to the mixing chamber length, whereas the starting pressure of conventional central injection supersonic ejectors obeys normal shock theory, because the mixing chamber of the annular injection supersonic ejector is relatively longer than that of conventional ejectors. When the mixing chamber length is short enough, the starting pressure of the annular injection supersonic ejectors also satisfies the normal shock theory. This indicates that there is a critical length, and the dependency of the starting pressure is divided by the critical length.

In the present study, the complex dependency of the starting pressure on the mixing chamber length is described by a simple model that employs the first series of diamond-shaped wave patterns of an overexpanded flow and an empirical factor. Using the model, a diagram of correlation between the minimum stagnation pressure and the mixing chamber length was obtained. From this diagram, the minimum stagnation pressure to start an ejector was estimated for a given mixing chamber length. The predicted minimum pressure showed good agreement with the measurements. The diagram also revealed the hysteresis behavior of a supersonic ejector by predicting different stagnation pressures of the primary flow that starts and unstarts the ejector. The critical length that was anticipated by previous measurements was defined as the intersection of the chamber length predicted by the normal shock theory and the length predicted by an analysis of the present model.

The empirical factor, S, results from considering the repetition of the diamond-shaped wave patterns, and various physical phenomena that have not been adequately accounted for in this simplified model are included, that is, the contraction angle at the mixing chamber inlet, wall friction, and the supersonic–supersonic interaction. The S factor is almost constant for similar sizes, such as the inner diameter at the primary nozzle exit, because all of these physics are strongly dependent on size, especially in an internal flow. The factor does not change dramatically in a small size. However, in larger dimensions, we can imagine that the S factor is smaller than that of the smaller dimensions. Because the effects of the contraction angle at the inlet of the mixing chamber and wall friction are small, the overexpanded flow can develop easily.

Table 3 Critical length of mixing chamber

Primary Mach number	Critical length, mm		Error, %
	Kim et al. [3]	Analysis	
3.8	66.8	66.2	−0.9
4.0	67.1	65.7	−2.1
4.2	67.8	68.4	0.9

Acknowledgment

This work was supported by Korea Science and Engineering Foundation (KOSEF) grant no. R01-2006-000-11311-0, funded by the Korean Ministry of Science and Technology.

References

[1] Sun, D. W., and Eames, I. W., "Recent Developments in the Design Theories and Applications of Ejectors—A Review," *Journal of the Institute of Energy*, Vol. 68, No. 5, Sept. 1995, pp. 65–79.

[2] Keenan, J. H., Neumann, E. P., and Lustwerk, F., "An Investigation of Ejector Design by Analysis and Experiment," *Journal of Applied Mechanics*, Vol. 72, No. 3, 1950, pp. 299–309.

[3] Kim, S., Jin, J., and Kwon, S., "Experimental Investigation of an Annular Injection Supersonic Ejector," *AIAA Journal*, Vol. 44, No. 8, Aug. 2006, pp. 1905–1908. doi:10.2514/1.16783

[4] Goethert, B. H., "High altitude and space simulation testing," *ARS Journal*, Vol. 32, No. 12, 1962, pp. 872–882.

[5] Goethert, B. H., "Simulated-Altitude Rocket Testing," *Astronautics*, Vol. 6, Jan. 1961, pp. 28–29, 40–42.

[6] German, R. C., Bauer, R. C., and Panesci, J. H., "Methods for Determining the Performance of Ejector-Diffuser Systems," *Journal of Spacecraft and Rockets*, Vol. 3, No. 2, 1966, pp. 193–200.

[7] Annamalai, K., Visvanathan, K., Sriramulu, V., and Bhaskaran, K. A., "Evaluation of the Performance of Supersonic Exhaust Diffuser Using Scaled Down Models," *Experimental Thermal and Fluid Science*, Vol. 17, No. 3, July 1998, pp. 217–229. doi:10.1016/S0894-1777(98)00002-8

[8] Annamalai, K., Satyanarayana, T. N. V., Sriramulu, V., and Bhaskaran, K. A., "Development of Design Methods for Short Cylindrical Supersonic Exhaust Diffuser," *Experiments in Fluids*, Vol. 29, No. 4, Oct. 2000, pp. 305–308. doi:10.1007/s003489900071

[9] Boreisho, A. S., Khailov, V. M., Malkov, V. M., and Savin, A. V., "Pressure recovery system for high power gas flow chemical laser," *XIII International Symposium on Gas Flow & Chemical Lasers—High Power Laser Conference*, International Society for Optical Engineering, Bellingham, WA, 2000, pp. 401–405.

[10] Malkov, V. M., Boreisho, A. S., Savin, A. V., Kiselev, I. A., and Orlov, A. E., "Choice of Working Parameters of Pressure Recovery Systems for High-Power Gas Flow Chemical Lasers," *XIII International*

Symposium on Gas Flow & Chemical Lasers—High Power Laser Conference, International Society for Optical Engineering, Bellingham, WA, 2000, pp. 419–422.

[11] Al-Najem, N. M., Darwish, M. A., and Youssef, F. A., "Thermovapor Compression Desalters: Energy and Availability—Analysis of Single- and Multi-Effect Systems," *Desalination*, Vol. 110, No. 3, 1997, pp. 223–238. doi:10.1016/S0011-9164(97)00101-X

[12] Kanada, T., and Kudo, K., "A Conceptual Study of a Combined Cycle Engine for an Aerospace Plane," AIAA Paper 2002-5146, 2002.

[13] Aoki, S., Lee, J., Masuya, G., Kanada, T., and Kudo, K., "Aerodynamic Experimental on an Ejector-Jet," *Journal of Propulsion and Power*, Vol. 21, No. 3, May–June 2005, pp. 496–503.

[14] Etele, J., Sislian, J. P., and Parent, B., "Effect of Rocket Exhaust Configurations on Ejector Performance in RBCC Engines," *Journal of Propulsion and Power*, Vol. 21, No. 4, July–Aug. 2005, pp. 656–666.

[15] Anderson, J. D., *Modern Compressible Flow with Historical Perspective*, 3rd ed., McGraw–Hill, New York, 2003, Chaps. 4, 5.

[16] Hodge, B. K., and Koenig, K., *Compressible Fluid Dynamics*, Prentice–Hall, Upper Saddle River, NJ, 1995, Chap. 6.

[17] Mikkelsen, C. D., Sandberg, M. R., and Addy, A. L., "Theoretical and Experimental Analysis of the Constant-Area, Supersonic–Supersonic Ejector," U. S. Army Research Office, Grant Number DAHC 04-75-G-0046, and Dept. of Mechanical & Industrial Engineering, Univ. of Illinois at Urbana-Champaign, Urbana, IL, 1976.

[18] Emanuel, G., "Optimum Performance for a Single-Stage Gaseous Ejector," *AIAA Journal*, Vol. 14, No. 9, 1976, pp. 1292–1296.

[19] Aksel, M. H., and Eralp, O. C., *Gas Dynamics*, Prentice–Hall, New York, 1994, Chap. 8.

E. Gutmark
Associate Editor